

Case History

Two- and three-dimensional electrical resistivity imaging at a heterogeneous remediation site

Laurence R. Bentley* and Mehran Gharibi*

ABSTRACT

Geometrically complex heterogeneities at a decommissioned sour gas plant could not be adequately characterized with drilling and 2D electrical resistivity surveys alone. In addition, 2D electrical resistivity imaging profiles produced misleading images as a result of out-of-plane resistivity anomalies and violation of the 2D assumption. Accurate amplitude and positioning of electrical conductivity anomalies associated with the subsurface geochemical distribution were required to effectively analyze remediation alternatives. Forward and inverse modeling and field examples demonstrated that 3D resistivity images were needed to properly reconstruct the amplitude and geometry of the complex resistivity anomalies. Problematic 3D artifacts in 2D images led to poor inversion fits and spurious conductivity values in the images at depths close to the horizontal offset of the off-line anomaly. Three-dimensional surveys were conducted with orthogonal sets of Wenner and dipole-dipole 2D resistivity survey lines. The 3D inversions were used to locate source zones and zones of elevated ammonium. Thus, conducting 3D electrical resistivity imaging (ERI) surveys early in the site characterization process will improve cost effectiveness at many remediation sites.

INTRODUCTION

Electrical resistivity imaging (ERI) has become an important engineering and environmental site investigation tool. Resistivity images are created by inverting hundreds to thousands of individual resistivity measurements (e.g., Loke and Barker, 1996a,b) to produce an approximate model of the subsurface resistivity. In most investigations, ERI data are collected along

transects. During the inversion step, resistivity in the cross-line direction is assumed constant. At sites with complex resistivity structure, the 2D assumption may introduce significant error, and the resulting 2D images can contain significant distortions.

Loke and Barker (1996a) have used 3D ERI with a pole-pole array to image sand channels in a 3×3 -m block. They conclude that, in this situation, 2D resistivity surveys are probably not adequate to properly image the subsurface. Chambers et al. (1999) have conducted a 3D ERI survey over oil- and tar-contaminated soils. Their survey covers a 95×95 -m area with orthogonal sets of colinear pole-dipole arrays. The survey was motivated by discrepancies between 1D and 2D geophysical data and ground truthing. Ogilvy et al. (1999) have conducted 3D ERI surveys over an old quarry site used as a landfill. Their survey, consisting of five parallel lines collected in the pole-dipole configuration, was conducted in three dimensions because the heterogeneity of the site precluded the use of 2D arrays. Park (1998) uses time-lapse 3D ERI to track fluid infiltration. He conducts a pole-pole survey with an array of 25 electrodes covering a 200×200 -m area. His results contain artifacts in the models and lack independent verification of the ERI results. Brunner et al. (1999) image a deep Tertiary maar structure using three concentric rings of electrodes and dipole-dipole measurements, imaging to depths of 900 m over an areal extent of 3 km^2 . The results are consistent with an independent gravity interpretation. Li and Oldenburg (1994) use the E-SCAN method to image an epithermal area associated with mineral deposits. A 35×35 grid with electrode spacing of 91.4 m produces 3D images with depths to 600 m. Slater and Binley (2003) use cross hole 2D and 3D induced polarization and resistivity images to investigate the integrity of permeable reactive barriers. They conclude that 2D imaging is sufficient over most of the barrier but that 3D imaging would improve the assessment of the ends of the barrier and might be required to assess the variability in the barrier at a finer scale. Chambers et al. (2002) use orthogonal sets of dipole-dipole and Wenner

Manuscript received by the Editor May 29, 2002; revised manuscript received December 29, 2003.

*University of Calgary, Department of Geology and Geophysics, Calgary, Alberta T2N 1N4 Canada. E-mail: lbentley@ucalgary.ca; mgharibi@ucalgary.ca.

© 2004 Society of Exploration Geophysicists. All rights reserved.

1D lines to image known targets at an experimental site. They conclude that the 3D inversions are superior to quasi-3D images produced from sets of 2D inversions.

We collected resistivity images as part of a remediation research program at a decommissioned sour gas processing plant. Remediation options such as soil removal, in-situ degradation, and phytoremediation were being studied to determine the most cost-effective approaches to dealing with the soils and groundwater at sour gas plant sites. Resistivity imaging was being used to identify areas of concern and to help develop a detailed picture of subsurface conditions. As with the previously cited authors, we concluded that site heterogeneity causes the 2D images to be affected by 3D geometric effects of the site's electrical conductivity heterogeneities. The 2D images indicate several features inconsistent with other data collected at the remediation site and with our understanding of the geological and geochemical distributions across the site. The 2D images could not be used to locate obvious anomalies and, in some instances, led to incorrect interpretations.

In the following case history, we demonstrate how 3D geometric effects can contaminate and distort 2D images. We use forward and inverse modeling to demonstrate positioning and imaging issues. A practical 3D survey design is described. Results from 2D and 3D surveys are compared and discussed in relation to field validation and the forward modeling results. We discuss some of the resolution issues associated with our 3D design. Finally, we conclude that 3D surveying may be the most cost-effective surveying method in some field situations.

SITE DESCRIPTION

The study was conducted on the site of a decommissioned sour gas processing plant in central Alberta (Figure 1). The site is located on a topographic high that is surrounded on three sides by steep slopes. North of the site, the topography slopes gently upward for about 200 m and then descends another steep slope into a ravine.

The site is underlain by discontinuous Quaternary till which overlies Tertiary sandstone and siltstone rocks. Generally, the surficial material consists of an uneven layer of fill, broken concretes, and other material to a depth of 1 m. Below the fill is a layer of olive-brown till with sand lenses which extends to 3.5 m below ground level. At 3.5 m, the olive-brown till grades into a cohesive dark-brown clay till that extends down to 6 m. Underlying the dark-brown clay till is gray silt till with occasional bedrock fragments. An uneven, weathered bedrock surface is found between 6 and 9 m below ground level.

The site is undergoing remediation. All of the surface facilities with the exception of a small shed have been removed. Gas was processed on the site using amine and glycol compounds to remove the water, carbon dioxide, and hydrogen sulfide. These compounds were released over the course of many years during plant operations. Amine degrades to ammonium and acetic acid, and glycol degrades to acetic acid (Mrklas, 2002; Ndegwa et al., 2004). The amine, ammonium, and acetic acid increase the electrical conductivity of soil water and cause zones of elevated bulk electrical conductivity in the subsurface.

Extensive investigations had been conducted at various locations across the site prior to the 3D ERI surveys. Drilling, piezometer installations, push tool conductivity (PTC) surveys,

and 2D ERI demonstrated that soil and water quality varied over horizontal distances on the order of 1 m and that zones of high electrical conductivity were as thin as 0.5 m in the vertical. Most of the elevated concentrations are within 6 m of the surface.

2D ERI IN HETEROGENEOUS FORMATIONS

Previous 2D ERI surveys indicated localized high electrical conductivity anomalies. Lines 10r2 and 02r2 were imaged using a linear array of electrodes separated by 1 m and the Wenner configuration (Figure 1). Electrical conductivity values above background levels were observed on line 10r2 near PTC 03 (Figure 2a) and on line 02r2 near PTC 22 (Figure 2c). Figure 3a shows the laboratory-measured electrical conductivity of core taken near PTC 03 and the electrical conductivity-depth profile of PTC 03. The electrical conductivity of the two depth profiles are consistently near or below 100 mS/m. However, an electrical conductivity-depth profile from line 10r2 at the same horizontal location shows an electrical conductivity of nearly 400 mS/m at around 886 m elevation. Similarly, the electrical conductivity-depth profile from PTC 22 is consistently just over 100 mS/m, but at the same location the electrical conductivity-depth profile from line 02r2 shows values on the order of 300 mS/m for elevations below 884 m (Figure 3b). A geotextile liner near line 02r2 had been installed previously to impede groundwater flow to the southeast (Figure 1). The liner is an electrical insulator, and it is the shallow resistive feature at PTC 22 (Figure 2c). We suspected that the deeper conductive feature seen below the liner was from conductive ground located behind the liner. These contradictions in the data sets

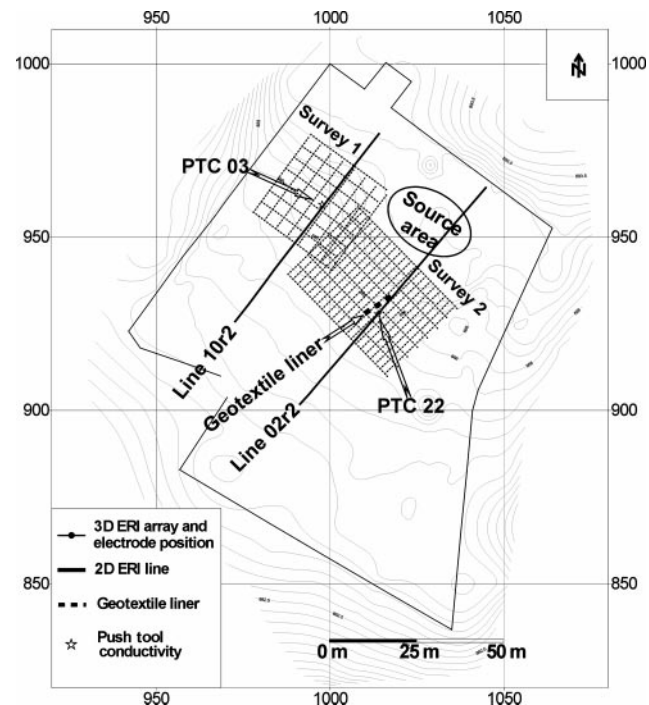


Figure 1. Location map. Survey 1 consists of eight northwest-southeast lines and eight southwest-northeast lines. The dipole-dipole array was used in both directions. Survey 2 includes eight northwest-southeast lines using a Wenner array and twenty-one southwest-northeast lines using a dipole-dipole array.

and the other indications of extreme heterogeneity within the subsurface electrical conductivity indicated that out-of-plane anomalies were yielding ambiguous and often misleading ERI images.

MODEL EXAMPLE OF 2D VERSUS 3D IMAGING

To demonstrate the process and magnitude of 3D structure effects on 2D ERI surveys, 3D numerical modeling was conducted using a synthetic model with grid size of $31 \times 31 \times 10$ (Figure 4a). The model consisted of a conductive anomalous block with 4-m lateral extent located at the center of the model between 0.8 and 2.6 m depth. The conductivity of the anomaly was 1000 mS/m, and it was embedded in a resistive homogeneous half-space with conductivity of 10 mS/m. The geometry

and conductivity contrasts of the resistivity model were similar into those found at the gas plant site. Using the finite-difference (FD) method (Loke and Barker, 1996a), we calculated the 3D resistivity responses for a theoretical survey. A series of 31 dipole-dipole lines separated by 1 m was simulated in the *x*-direction, with another 31 lines in the *y*-direction. Each line consisted of 31 electrode locations separated by 1 m.

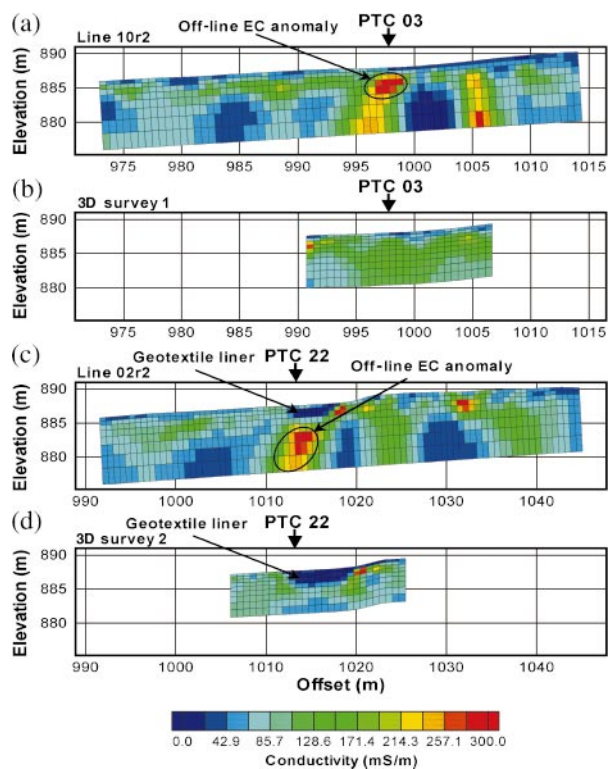


Figure 2. ERI profiles with locations of PTC profiles. (a) ERI line 10r2 with out-of-plane artifact. (b) Profile at line 10r2 extracted from the 3D ERI of survey 1. (c) ERI line 02r2 with out-of-plane artifact. (d) Profile at line 02r2 extracted from the 3D ERI of survey 2.

Figure 3. Comparison of electrical conductivity from PTC, core, and ERI-derived. (a) PTC vertical profile 03, core, conductivity values from the same location from 2D (line 10r2), and 3D (survey 1) inversions. (b) PTC vertical profile 22 with conductivity values from the same location derived from 2D (line 02r2) and 3D (survey 2) ERI inversions. The 2D lines show anomalously high values of resulting from out-of-plane anomalies. The 3D inversions are more consistent with core and PTC data.

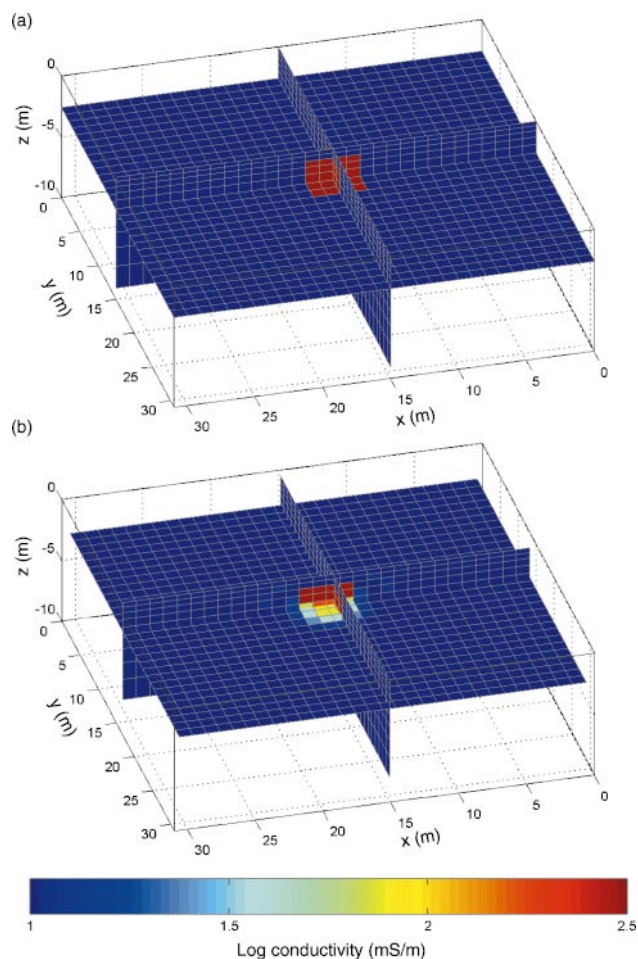
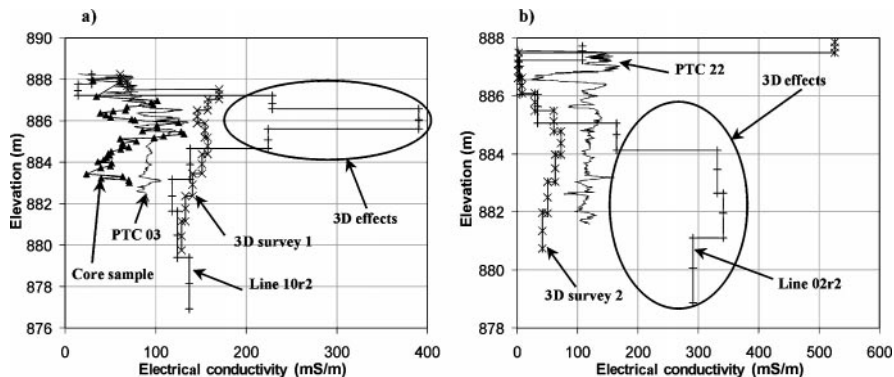


Figure 4. Hypothetical conductivity model and 3D inversion results. (a) Model of high-conductivity feature embedded in a resistive background. (b) Results of a 3D inversion of a simulated survey calculated with forward modeling using the conductivity model from (a).

The apparent resistivity data from both sets of lines were jointly inverted using a 3D resistivity inversion code (Loke and Barker, 1996a) with $31 \times 31 \times 11$ elements and 10 571 model parameters. Figure 4b shows the results of the inversion. The high-conductivity body has been located correctly. The electrical conductivity in the image near the bottom of the body is somewhat low, and a slight halo of elevated electrical conductivity surrounds the body. The halo and reduced electrical conductivity are consistent with smoothing used to stabilize the inversion. Figure 5a shows cross-sections from the 3D inversion at 3, 7, 11, and 15 m offset along the x -axis (i.e., in the y - z plane). The cross-sections at 3, 7, and 11 m correctly reproduce the background conductivity with no indication of the high-conductivity body. The cross-section at 15 m, which cuts across the center of the anomalous body, has successfully imaged the geometry and magnitude of the conductive anomaly. The top and sides of the conductive block are well resolved. Again, the value of electrical conductivity along the lower boundary of the block is underpredicted, and a slight halo of high-conductivity is visible around the body. However, the results give a good estimation of the location of the lower boundary and the scale of the conductive anomaly.

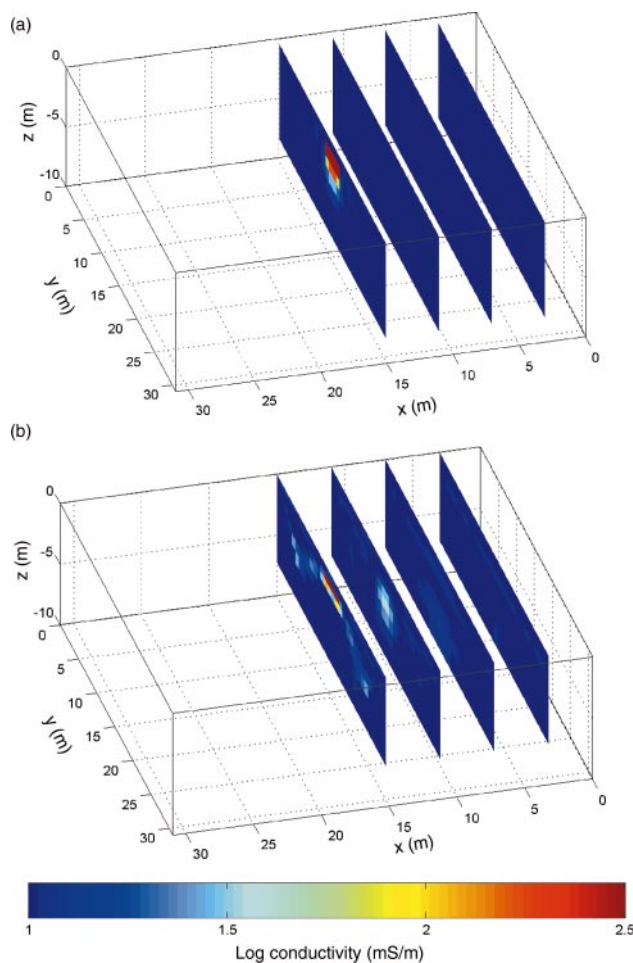


Figure 5. Selected profiles of electrical conductivity. (a) Selected planes from the 3D inversion shown in Figure 4b. (b) The 2D inversions of simulated 2D lines. The inversion results show obvious incorrect amplitudes and positioning of the 3D anomaly.

A set of 2D ERI lines along the electrodes at 3, 7, 11, and 15 m offset along the x -axis was extracted from the 3D ERI model response data set. These profiles, simulating a dipole-dipole array with 31 electrodes and 1-m electrode spacing, were individually inverted using a 2D ERI inversion code (Loke and Barker, 1996b); the results are shown in Figure 5b. Again, the profile located at 15 m crosses the center of the conductive anomaly, and the other three profiles are offset 10, 6, and 2 m distant from the closest face of the body. The profile at 3 m correctly estimates the true conductivity of the background. Spurious features or 3D effects are not observed. The reason is that the off-profile anomalous body is out of the maximum depth of penetration of the data in this profile (about 7 m). The profile located at 7 m has a slightly elevated electrical conductivity of 13 mS/m below the depth of about 6 m. The offline high-conductivity body is projected to a depth equal to the horizontal offset. This effect is repeated and is stronger on the image from the profile located at 11 m. On that profile, a conductive anomaly of up to 40 mS/m appears at a depth of about 3 m beneath the survey line. The results from these three profiles show that the magnitude and depth of the off-profile anomalies' effects depends on the distance from the profile plane and the depth of the anomalous body. Smaller offset distances result in greater 3D effects at shallower depths.

The section at 15 m depicts the results of 2D inversion when the anomalous body has a finite dimension. The conductive block anomaly causes a prominent high-conductivity anomaly at a depth that is too shallow and too thin. The main body of the electrical-conductivity high is flanked by two dipping conductive features that are similar in depth and magnitude to the false anomalies appearing on the offset profiles at 7 and 11 m. Beneath the thin conductive anomaly, the electrical conductivity of the background is lower than the 10-mS/m background value. The poor imaging is the result of a violation of the 2D assumption used in the 2D inversion. The inversion process tries to match the potential distribution caused by a finite 3D body with a 2D conductive anomaly that extends to infinity in the cross-line direction. As a result, the reconstructed 2D model cross-section is thinner than the 3D body and has the large edge effects (Dahlin and Loke, 1997). The total rms misfits are 0.1%, 0.12%, 0.28%, and 14.66% for 2D profiles located at 3, 7, 11, and 15 m, respectively. The increasing rms errors indicate increasing violation of the 2D assumption and the decreasing reliability of the 2D images in the presence of the 3D heterogeneity. We infer that the large rms errors from inversions of noise-free data indicate the 2D model is not adequate to duplicate the observations. A large rms error in 2D ERI inversions should be viewed as a possible indication of significant 3D heterogeneity.

SURVEY DESIGN

ERI equipment

Survey design must take into account the capabilities of the acquisition system. The survey was conducted with a single-channel unit that automatically measures in a preprogrammed sequence of current and potential electrode pairs. Our system consisted of 56 electrode stations divided between four 14-electrode cables with 12-m maximum take-out separation. Depending on acquisition parameters, the system completes approximately six resistivity measurements per minute.

Design considerations

An electrode spacing of 1 m was considered an appropriate spacing, given the scale of electrical conductivity variations and the resolution requirements. Minimizing acquisition time reduces costs and complications that arise because of changing environmental conditions. In particular, an inversion would suffer if the electrical conductivity in part of the survey area changed during the survey. For example, a thunderstorm could increase soil moisture and thereby the electrical conductivity of the near surface. Consequently, we required an acquisition strategy that used 1-m electrode arrays but could be completed in a day or two.

Pole-dipole (Chambers et al., 1999; Ogilvy et al., 1999), pole-pole (Loke and Barker, 1996a; Park, 1998), and E-SCAN (Li and Oldenburg, 1994) 3D ERI surveys have been reported. However, these methods were impractical because of the length of the cables, the number of electrodes, site geometry, and the 1-m electrode spacing. In contrast, Chambers et al. (2002) used sets of 2D lines to construct 3D surveys. Sets of 2D lines allow flexible survey design and are easily adaptable to our system.

In this case history, we report on the results of two 3D surveys with different designs. Both designs use orthogonal sets of 2D lines. A systematic bias in the current and potential measurement directions may lead to grid orientation effects (Dahlin et al., 2002; Chambers et al. 2002). Orthogonal lines were used to reduce potential grid orientation effects. The Wenner and dipole-dipole arrays were used. The Wenner array has better depth resolution, less susceptibility to acquisition noise, and fewer measurement points for the same line coverage than the dipole-dipole array (Ward, 1990). The dipole-dipole array has better horizontal resolution and better depth coverage at the ends of the lines.

Survey 1 was conducted with orthogonal sets of 27-m-long 2-D profiles (Figure 1). The survey consisted of eight northwest-southeast dipole-dipole lines and eight northeast-southwest dipole-dipole lines. Lines were separated by 4 m.

Analysis of the survey 1 results suggests that the 4-m line spacing was too coarse to capture the more complicated near-surface electrical conductivity distribution anticipated in the survey 2 area. In addition, the survey 2 region was larger. Consequently, survey 2 was conducted with 21 southwest-northeast dipole-dipole profiles that were 27 m long and separated by 2 m. Eight orthogonal Wenner array profiles that were 41 m long were acquired with 4-m line separation. The 2-m line separation improved the resolution in the near surface, and the use of the Wenner array on the longer lines reduced the acquisition time because fewer measurements were used per line than with the dipole-dipole array.

All lines used an electrode spacing of 1 m. Lines collected with the dipole-dipole array used dipole a -spacings varying from 1 to 3 m. The maximum distance between the current pair and the potential pair of electrodes was limited to a maximum of $n = 6$ a -spacings. Larger interdipole spacings led to unacceptable levels of noise in the data. Lines collected with the Wenner array used a -spacings from 1 to 17 m.

FIELD PROCEDURES

The ends of each line and line intersections were located with survey equipment to provide horizontal position and elevation

control. Electrodes that were not located on the line intersections were positioned with a survey chain. For the dipole-dipole lines, the electrodes were positioned and attached to the cable while acquiring the previous line. Transition between acquisition lines was limited to a quick movement of the recording equipment and a contact resistance test. Once the automated data acquisition commenced, each dipole-dipole line took approximately 30 min to record and each Wenner line took approximately 45 min. A four-person crew was needed for continuous recording. Each measurement was repeated three times. Repeated measurements with rms variation greater than 1% were rejected.

RESULTS

Resistivity data were inverted with the RES3DINV program (Loke and Barker, 1996a). The finite-element option was used to account for elevation variations across the site. The inversion results have an rms error of 7.93 and 4.01 for surveys 1 and 2, respectively.

Inversion results for 3D survey 1 are shown in Figure 6. Background electrical conductivity is 60 to 100 mS/m. Three distinct localized electrical conductivity highs are seen in Figure 6. The first is a small localized high 0.2 m below ground level in the southwest portion of the image. The anomaly is located in one of the square regions of no coverage between the orthogonal line sets. No source for this localized anomaly of high electrical conductivity was located, and it may be an artifact caused by poor control in the upper layers of the image as a result of the coarse line spacing.

Another electrical conductivity high is seen between 1.0 and 1.5 m below ground level in the southeast. This electrical conductivity high had been detected by a 2D ERI line not discussed here but had not been located previously because it was located northwest of the 2D line. Based on the 3D ERI results, the location was excavated. The soil contained elevated concentrations of ammonium. Tests on two soil samples from this zone showed 331 and 366 mS/m, and the ERI inversion in the area of the anomaly yielded values of 242 to 790 mS/m.

The third anomaly is seen between 1.5 and 3.0 m. This anomaly corresponds to the electrical conductivity high seen in line 10r2 near PTC 03 (Figure 2a). Figure 2b is an extracted profile from the 3D inversion along the location of line 10r2; in contrast to the 2D inversion, the 3D inversion has no indication of electrical conductivity at this location. The electrical conductivity-depth profile from the 3D image at PTC 03 has values slightly higher than the values from the PTC and core but generally conforms with the trends shown by these measurement (Figure 3a). The 3D profile does not show elevated electrical conductivity at 886 m elevation. An excavation at the site of the third anomaly verified the position and depth of the anomaly. Discolored soil corresponded to the location of the anomaly, and soil tests indicated detectable amine, elevated ammonium, and elevated acetic acid. Electrical conductivity from a soil sample was 824 mS/m, compared with 600 to 3000 mS/m from the ERI inversion.

The inversion results from 3D survey 2 are shown in Figure 7. The zone of high electrical conductivity between the surface down to 2.1 m is evident and is consistent with environmental studies performed on the site. The location of the geotextile liner is apparent on the images and separates the extensive

region of high electrical conductivity from the eastern lower electrical conductivity region. Line 02r2 passes to the east of the liner, explaining the inconsistency between the results of line 02r2 and PTC 22 (Figure 3b). A profile along line 02r2 extracted from the 3D inversion results shows no evidence of the electrical-conductivity high imaged in Line 02r2 (Figure 2d). In addition, the liner is better resolved and is seen to be deeper in the 3D image, consistent with the construction. Again, the electrical conductivity–depth profile extracted from the 3D volume shows much better agreement with the PTC22 profile than the 2D inversion results (Figure 3b). However, the ERI image

above 886 m underestimates the value of the electrical conductivity because of the close proximity of the geotextile liner.

CONCLUSIONS

Three-dimensional electrical resistivity can be a practical tool for resolving of complex subsurface heterogeneity. In the case of the gas plant site, locating all targets was close to impossible using drilling and 2D ERI surveying alone because of the complex 3D nature of the chemical distribution in the subsurface. Modeling results illustrate the interpretation problems associated with 2D ERI. In particular, out-of-plane effects

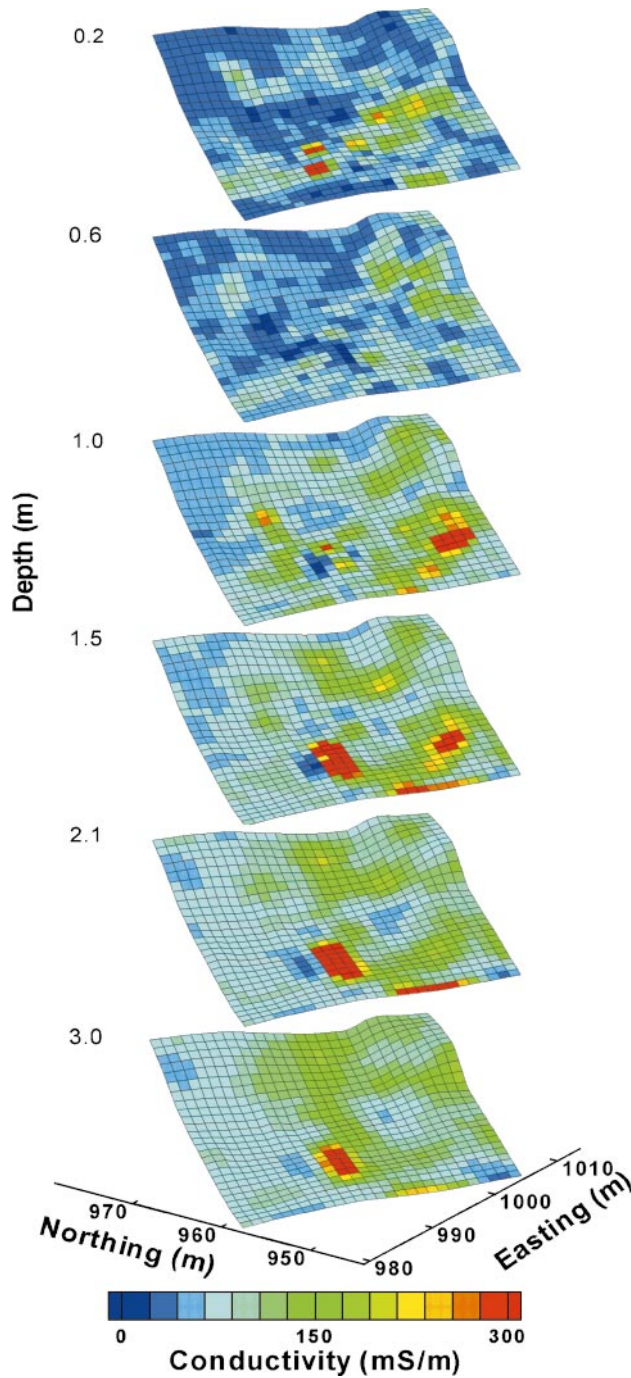


Figure 6. Electrical conductivity from 3D inversion of survey 1.

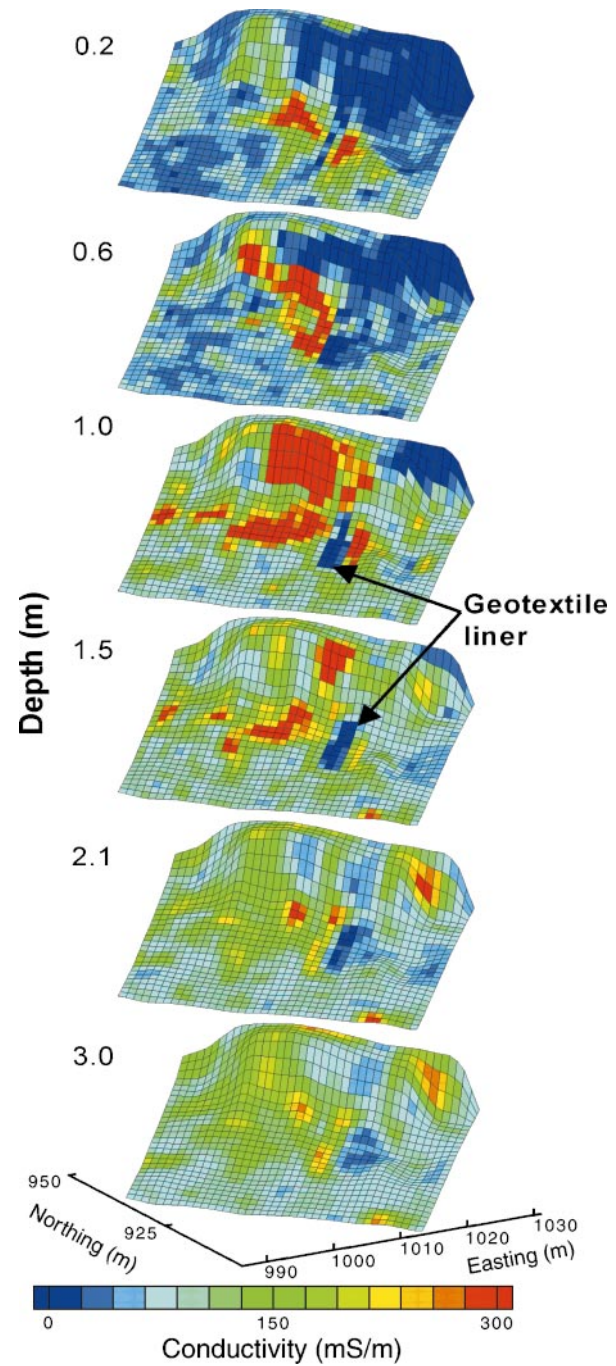


Figure 7. Electrical conductivity from 3D inversion of survey 2.

led to incorrect location of PTC surveys and piezometers. The amplitude as well as the location of the 2D-derived electrical conductivity anomalies was incorrect.

A map of the source areas and areas of high concentration of ammonium and degradation byproducts is needed to compare the efficacy and cost associated with remediation alternatives. Other studies indicate that locations with electrical conductivity values greater than 154 mS/m are possible source areas and possible high concentrations of ammonium, and that areas with electrical conductivity greater than 224 mS/m always have high ammonium concentrations. By defining the areas of high electrical conductivity, the cost associated with source removal and the associated overburden can be estimated. Since high concentration of ammonium in the soil may inhibit plant growth, locating the boundaries of electrical conductivity greater than 224 mS/m helps in the design of phytoremediation programs. Consequently, the correct location of electrical conductivity anomalies and correct electrical conductivity values are needed to effectively use ERI to evaluate remediation alternatives. At this site, 3D surveys were needed to provide the correct locations and magnitudes of electrical conductivity values.

Three-dimensional surveys can be constructed with orthogonal sets of 2D lines. The method is simple to administer, and data can be collected in a reasonable amount of time. In this study, in-line electrode spacing was 1 m and cross-line spacing was either 2 or 4 m. The dense in-line spacing allowed us to capture the detailed heterogeneity, and the larger cross-line spacing yielded an acceptable acquisition time. Large line separation does compromise the resolution of portions of the near-surface layers because the rectangular areas between the lines are not adequately sampled by the shortest offset arrays.

This study illustrates the importance of identifying artifacts associated with 3D effects early in a characterization campaign. Two-dimensional inversion profiles with high rms fitting errors and unexplained anomalies in the lower part of the sections should be investigated. We estimate the commercial cost of acquiring and processing the 42 × 28-m survey (survey 2) to be equivalent to the cost of drilling and installing six piezometers at this site. Clearly, six piezometer installations could not capture the complexity evident in Figure 7. Similarly, survey 1 successfully located small pockets of elevated electrical conductivity associated with the target compounds and significantly lowered the risk and liability associated with nondetection. If 3D surveys are conducted early in the site assessment process, piezometers can be strategically located, reducing the total number of piezometers required at the site and lowering the cost of installation and water chemistry anal-

ysis. At contamination sites, reduced drilling reduces the risk of cross-contamination and reduces the cost of decommissioning piezometers at the end of remediation. Finally, the 3D survey can reduce the time required for site assessment, improve the accuracy of the characterization, and possibly reduce the total cost of characterization. Consequently, conducting 3D ERI surveys early in the site characterization process will be cost effective at many sites.

ACKNOWLEDGMENTS

We thank Imperial Oil Resources for logistical, technical, and financial support. Funding was also provided by the Natural Sciences and Engineering Research Council of Canada.

REFERENCES

- Brunner, I., Friedel, S., Jacobs, F., and Danckwardt, E., 1999, Investigation of a Tertiary maar structure using three-dimensional resistivity imaging: *Geophysical Journal International*, **136**, 771–780.
- Chambers, J. E., Ogilvy, R. D., Kuras, O., Cripps, J. C., and Meldrum, P. I., 2002, 3D electrical imaging of known targets at a controlled environmental test site: *Environmental Geology*, **41**, 690–704.
- Chambers, J., Ogilvy, R., Meldrum, P., and Nissen, J., 1999, 3D Resistivity imaging of buried oil- and tar-contaminated waste deposits: *European Journal of Environmental and Engineering Geophysics*, **4**, 3–15.
- Dahlin, T., and Loke, M. H., 1997, Quasi-3D resistivity imaging—Mapping of three dimensional structures using two-dimensional DC resistivity techniques: 3rd Meeting, Environmental and Engineering Geophysics, Expanded Abstracts, 143–146.
- Dahlin, T., Bernstone, C., and Loke, M. H., 2002, A 3-D resistivity investigation of a contaminated site at Lernacken, Sweden: *Geophysics*, **67**, 1692–1700.
- Li, Y., and Oldenburg, D. W., 1994, Inversion of 3-D DC resistivity data using an approximate inverse mapping: *Geophysical Journal International*, **116**, 527–537.
- Loke, M. H., and Barker, R. D., 1996a, Practical techniques for 3D resistivity surveys and data inversion: *Geophysical Prospecting*, **44**, 499–523.
- 1996b, Rapid least-squares inversion of apparent resistivity pseudo-sections using quasi-Newton method: *Geophysical Prospecting*, **44**, 131–152.
- Mrklas, O., 2002, Ethanolamine and glycol biodegradation: From detection to remediation: Ph.D. dissertation, University of Calgary.
- Ndegwa, A. W., Wong, R. C. K., Chu, A., Bentley, L. R., and Lunn, S. R. D., Degradation of monoethanolamine in soil: *Journal of Environmental Engineering and Science*, **3**, 137–145.
- Ogilvy, R., Meldrum, P., and Chambers, J., 1999, Imaging of industrial waste deposits and buried quarry geometry by 3-D resistivity tomography: *European Journal of Environmental and Engineering Geophysics*, **3**, 103–113.
- Park, S., 1998, Fluid migration in the vadose zone from 3-D inversion of resistivity monitoring data: *Geophysics*, **63**, 41–51.
- Slater, L., and Binley, A., 2003, Evaluation of permeable reactive barrier (PRB) integrity using electrical imaging methods: *Geophysics*, **68**, 911–921.
- Ward, S. H., 1990, Resistivity and induced polarization methods, *in* Ward, S. H., Ed., *Geotechnical and environmental geophysics*, **1**: Society of Exploration Geophysicists, 147–189.